PHASE SPACE ANALYSIS AT THE SwissFEL INJECTOR TEST FACILITY

B. Beutner, R. Ischebeck, T. Schietinger
Paul Scherrer Institut, 5232 Villigen PSI, Switzerland

Abstract

Phase 1 of the SwissFEL Injector Test Facility consists of a 2.6-cell S-band RF gun, a spectrometer, and a series of transverse beam diagnostic systems such as YAG screens, slit and pepper-pot masks. Its primary purpose is the demonstration of a high-brightness electron beam meeting the specifications of the SwissFEL main linac. Phase space characterization at beam energies up to 7 MeV, where space charge still dominates, is performed with YAG screens in combination with slit- and pinhole (pepper-pot) masks. Advanced image analysis is used to mitigate artefacts due to background, pixel readout noise, or dark current. We present our data analysis procedure for the slit scan method, with particular emphasis on image processing and its effect on the reconstructed emittance. Pepper-pot measurements using an independent analysis framework are used to cross-check the slit scan results.

INTRODUCTION

SwissFEL Injector Test Facility

In preparation for the SwissFEL [1] project an injector test facility is presently being commissioned at PSI. In the final phase it will consist of an S-band RF gun, four S-band accelerating traveling wave structures, an X-band system for phase space linearization, a movable girder bunch compressor, and two transverse deflecting cavity systems for longitudinally resolved measurements. It will nominally reach energies of about 250 MeV with bunch charges of 200 pC. A detailed description of the SwissFEL Injector Test Facility can be found in [2] and [3].

One part of the mission of the 250 MeV Injector test facility is to demonstrate the production and transport of low emittance beams. For this purpose a series of emittance measurement diagnostic systems are foreseen. In the low energy part (below 100 MeV) a series of vertical and horizontal slit masks in different sizes (20 and 50 μm width) and a pinhole array ("pepper-pot") are installed. A FODO section has been designed to establish the required parameters above 100 MeV.

In this paper we discuss the analysis of emittance measurements obtained with the slit mask. High energy emittance measurements are conceptually different, they are discussed in [4]. The high-resolution profile monitor systems including YAG screens, which are used for these measurements, are described in [5]. First commissioning results as well as data from emittance studies are summarized in [6].
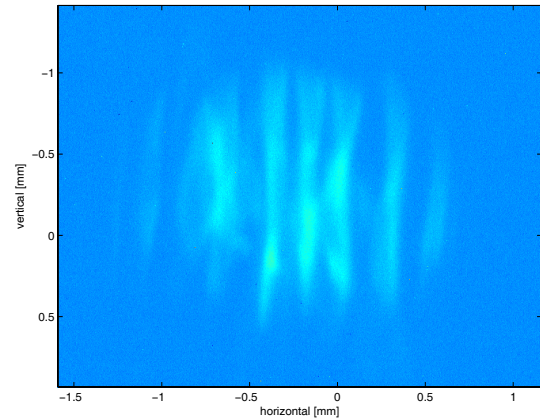

Figure 1: Summary of an example slit scan. For this image all images for different slit positions are superimposed.

Slit Scan

The main idea of a slit-scan (or a pinhole-array) emittance measurement is a position resolved measurement of beam divergence and transverse momentum of subsets of the beam which allows a reconstruction of the phase space. With a slit mask (or a pinhole array) a beamlet is created, which is then imaged on a downstream screen. From the beamlet position on the screen and the spot size the divergence and the beam moments can be determined. From the profiles of these images a reconstruction of the phase space distribution is possible. For details we refer to [7]. A typical slit scan is shown in Fig. 1.

An important step in such measurements is the determination of the beam sizes and profiles. Image artefacts due to background, pixel readout noise, or dark current can reduce the accuracy of such profile measurements. Therefore offline image analysis techniques are required.

IMAGE PROCESSING

The first standard step in each image analysis is the subtraction of the background. In our system we block the photo-cathode laser and record a series of images from the screen. The average of these images is then subtracted from all beam images. This procedure removes static (images of screen holders or scratches on the crystals) as well as dynamic (dark current) features from the image. Because of this dynamic contribution we repeat the background subtraction for every position of the slit mask.

Noise Cut

After background subtraction the remaining problem is the readout noise from the CCD or pixel illuminated by stray radiation. It leads to excited pixels over the entire image. Noise in the outer regions of the screen is not beam related. Since Gaussian fits to the profiles are sensitive to this noise and the beamlet shapes are in general not Gaussian, we introduce an additional step of image cleaning.

The idea is to mask parts of the image which are not related to the beam, removing noise contributions from these regions. A detailed summary of the method is given in [4]. This masking procedure is controlled by a single number, called threshold parameter. A low value of the threshold parameter corresponds to a large mask including some non-beam-related noise while a higher value reduces the area of the mask, eventually cutting contributions from the beam.

In a following step the average pixel intensity of the masked region is subtracted from the whole image to remove remaining offsets and then all masked parts are set to zero. An example of the image processing procedure is given in Fig. 2.

Threshold Scan

The described method for noise reduction in the profiles works well to obtain RMS values from the real CCD readout provided that the threshold parameter is set to some optimal value. The determination of this value, however, is crucial since the calculated emittance value depends on it. In Fig. 3 the reconstructed emittance of a typical measurement is plotted against the value of the threshold parameter. A clear dependence is observable. After a region of strong variation in the emittance as a function of the threshold parameter at low values a relatively stable region is reached. In the region above a threshold value of about 1 (in this example) the emittance decreases while the mask gets smaller and smaller reducing the effective reconstructed beam divergence. A criterion is needed for an unambiguous choice of threshold parameter.

In Fig. 3 we observe that the sizes of the error bars depend on the threshold value as well. These errors are determined from the statistical variation of the images: The measurements we present contain a series of images for each slit position. These images are not averaged but the whole analysis is repeated for each image index. This means for example that the first image for each slit position is used to give one emittance value, then the second for a new emittance value and so on. The errors shown in Fig. 3 are the statistical variations from all these values.

This statistical error has two major contributions: firstly the fluctuations of the beamlet sizes and positions and secondly the contributions from the noise in parts of the image which are not related to the beam spot. Contributions from noise far away from the beam spot should be larger than the beam fluctuations since the noise is almost uncorrelated from shot to shot and its distance to the center-of-mass is larger. Our goal is the mitigation of this contribution. This
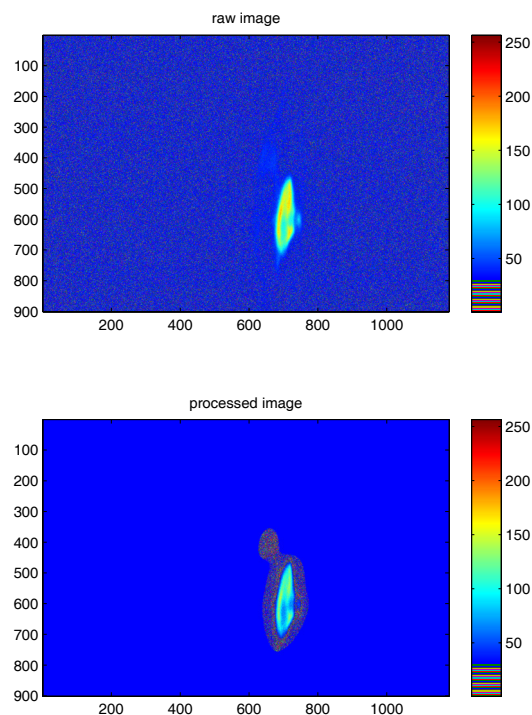

Figure 2: An example electron image of a 20 μm slit. The distance between slit and screen is 0.455 m. The upper image is the raw CCD readout. After image processing the lower image is obtained. The color map is adjusted to increase the visibility of the noise. Note that the color map is scaled to the maximum pixel intensity, which is different in each image. Axis labels are in pixels, the pixel size is 4.5 μm.

noise related error is expected to depend strongly on the threshold parameter since the masking will remove large parts of these fringe regions. The beam jitter contribution will only weakly depend on the threshold parameter. To summarize: the fluctuations (and thus the statistical error) will be large with a strong dependence on the threshold parameter if the CCD noise dominates or relatively small and constant in case the beam jitter dominates.

In Fig. 4 a detailed view of the transition region between these two regimes is given. The plot shows the reconstructed emittance and its error as a function of the threshold parameter. In this example the error below about 1.5 depends strongly on the threshold (noise dominated) while above that value the dependence is rather weak (beam-jitter dominated). The transition between these regimes is less pronounced in the emittance.

Our criterion for the choice of threshold parameter in emittance measurements now consists in selecting the lowest threshold value which still lies in the beam-jitter dominated regime, i.e., the lowest value for which the statistical
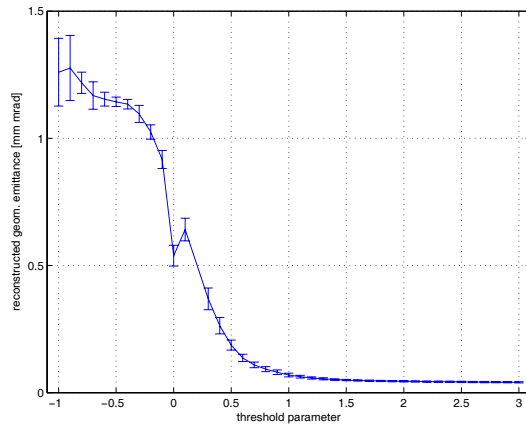
Figure 3: Emittance as a function of the threshold parameter. For low numbers the noisy regions of the image are still dominating the RMS beam parameters used for the emittance. The total reconstructed emittance drops down and reaches a relatively stable value for higher threshold parameters. After the strong decline of the reconstructed value an decrease of the error bar is visible. Figure 4 shows a detailed view of the threshold values between 1 and 3. Please note that the value of the threshold parameter can assume negative values due to the preceding background subtraction.

error is still stable. This is a good choice since higher values would cut parts of the beamlet spot, thus leading to an underestimation of the measured emittance.

CONCLUSION AND SUMMARY

We have presented a method of emittance analysis based on RMS beam size in combination with an image masking algorithm. A criterion is defined to arrive at a unique value of the emittance.

In the example presented above the analysis results in a geometric emittance of 0.050 ± 0.003 mm mrad. This result is consistent with an independent measurement and analysis done with a pepper pot (analysed with the Xana-ROOT tool [8]). A direct comparison is, however, difficult since the pinhole array and the slit mask are installed at different longitudinal positions, while the projected emittance may vary significantly after the gun. A detailed discussion of this comparison is beyond the scope of this paper.
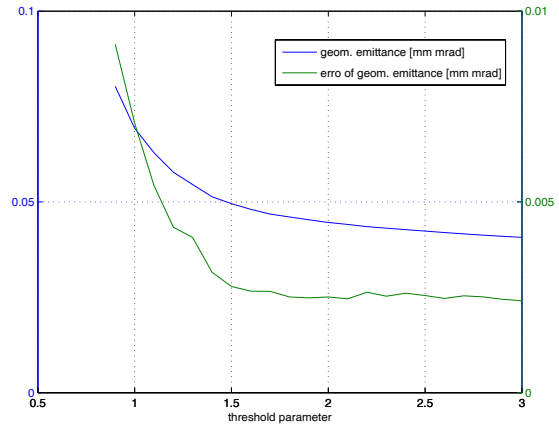

Figure 4: Reconstructed emittance as function of the threshold parameter and statistical error of the emittance. At a threshold value of about 1.5 the error stays relatively stable, which means that the effect of random CCD readout noise in non-beam-related parts of the image is minimized.

ACKNOWLEDGEMENTS

REFERENCES

[1] R. Ganter (ed.), "SwissFEL Conceptual Design Report", PSI report 10-04 (2010).

[2] M. Pedrozzi (ed.), "SwissFEL Injector Conceptual Design Report", PSI report 10-05 (2010).

[3] M. Pedrozzi et al., Proceedings of FEL'09 Conference, Liverpool, UK, (2009).

[4] B. Beutner, "Emittance Measurement Procedures for the SwissFEL 250 MeV Injector" , Proceedings of FEL09 Conference, Liverpool, UK (2009).

[5] R. Ischebeck et al., "Profile Monitors for the SwissFEL Injector Test Facility", Proceedings of LINAC10 Conference, Tsukuba, Japan (2010).

[6] T. Schietinger et al., "First Commissioning Experience at the SwissFEL Injector Test Facility", Proceedings of LINAC10 Conference, Tsukuba, Japan, 2010.

[7] S. Anderson et al., Phys. Rev. ST Accel. Beams 5 (2002) 014201.

[8] T. Schietinger, "XanaROOT: an Emittance Measurement Tool Based on ROOT", http://amas.web.psi.ch/XanaROOT.